Proc. Estonian Acad. Sci. Eng., 2004, **10**, 4, 281–289

https://doi.org/10.3176/eng.2004.4.06

Linear stability analysis of shear-flexible thin-walled beams

Domagoj Lanc, Goran Turkalj and Josip Brnić

Faculty of Engineering, University of Rijeka, Vukovarska 58, 51000 Rijeka, Croatia; {dlanc, turkalj,brnic}@riteh.hr

Received 1 July 2004, in revised form 17 September 2004

Abstract. This paper presents finite element based numerical stability analysis of thin-walled beam structures. Using the linearized virtual work principle with the assumption of large displacements, large rotations but small strains, a finite element equation is derived. Effects of cross-sectional shear deformations are also taken into account. To include large rotation effects, non-linear displacement field of the cross-section is used. A new two-node shear-flexible finite element with seven degrees of freedom per node is developed. Complete exact 14×14 elastic and geometric stiffness matrices are evaluated. An original computer program THINWALL-SHEAR is developed. Obtained results are compared with analytical and numerical results of other authors.

Key words: thin-walled beam, large displacements, large rotations, shear deformations.

1. INTRODUCTION

Tendency to optimize constructions and to reduce the production costs appeals for using thin-walled structures because they offer a high performance for a minimum weight. Complexity of their behaviour, especially from the point of view of the loss of stability, imposes numerical modelling because theoretical solutions are limited with cases of simple geometry.

Linear analysis treats stability as an eigenvalue problem and determines the critical load in a direct manner without calculating the deformations. The critical buckling load corresponds to the lowest eigenvalue and the corresponding eigen-vector represents the buckling mode. Such an analysis supposes an ideal structure and loading conditions, ignoring deformations before reaching the buckling load. Buckling load is considered to determine the load-carrying capacity.

Stability analysis, concerning large spatial rotation, is very complicated because of the non-vectorial nature of large rotations. Using standard linear

displacement field, torsional moment is of semitangential and bending moments are of quasitangential character; thus they induce non-compatible moments during large spatial rotations. In this work, non-linear displacement field is used which include large rotation effects. The derived geometric stiffness matrix of the finite element of the thin-walled beam includes all internal moments of semitangential character.

This work also assumes that the beam member is prismatic and straight, material is isotropic, cross-section is non-deformable in his own plane but it can warp, external loads are conservative and constitutive equations are linear.

2. BASIC CONSIDERATIONS

2.1. Non-linear displacement field

Cross-section displacements consist of seven components: three translational components w_o, u_s, v_s, three rotational components $\varphi_x, \varphi_y, \varphi_z$ and cross-sectional warping θ. In the right-handed Cartesian coordinate system (*z*, *x*, *y*), axis *z* coincides with the beam axis passing through the centroids O of the cross-sections. Coordinate axes *x* and *y* are the principal axes of inertia of the cross-section (Fig. 1).

Total displacement field is

$$\mathbf{U}_{uk}^{\mathrm{T}} = \{w + \tilde{w} \quad u + \tilde{u} \quad v + \tilde{v}\}, \tag{1}$$

where *w*, *u* and *v* are linear displacement field components:

$$w = w_o - y\varphi_x - x\varphi_y - \omega\theta, \qquad u = u_s - (y - y_s)\varphi_z, \qquad v = v_s + (x - x_s)\varphi_z, \tag{2}$$

and $\tilde{w}$, $\tilde{u}$ and $\tilde{v}$, are second-order components:

$$\begin{aligned} \tilde{w} &= \frac{1}{2}\left[\varphi_z\varphi_x(x - x_s) + \varphi_z\varphi_y(y - y_s)\right], \\ \tilde{u} &= \frac{1}{2}\left[\varphi_z^2 x_s + \varphi_x\varphi_y y - (\varphi_z^2 + \varphi_y^2)x\right], \\ \tilde{v} &= \frac{1}{2}\left[\varphi_z^2 y_s + \varphi_x\varphi_y x - (\varphi_z^2 + \varphi_x^2)y\right]. \end{aligned} \tag{3}$$

Using non-linear displacement field, the corresponding Green–Lagrange strain tensor is

$$\varepsilon_{ij} \cong e_{ij} + \eta_{ij} + \tilde{e}_{ij} \tag{4}$$

with components defined as [1]:

$$e_{ij} = \frac{1}{2}(u_{i,j} + u_{j,i}), \qquad \eta_{ij} = \frac{1}{2}(u_{k,i}u_{k,j}), \qquad \tilde{e}_{ij} = \frac{1}{2}(\tilde{u}_{i,j} + \tilde{u}_{j,i}). \tag{5}$$

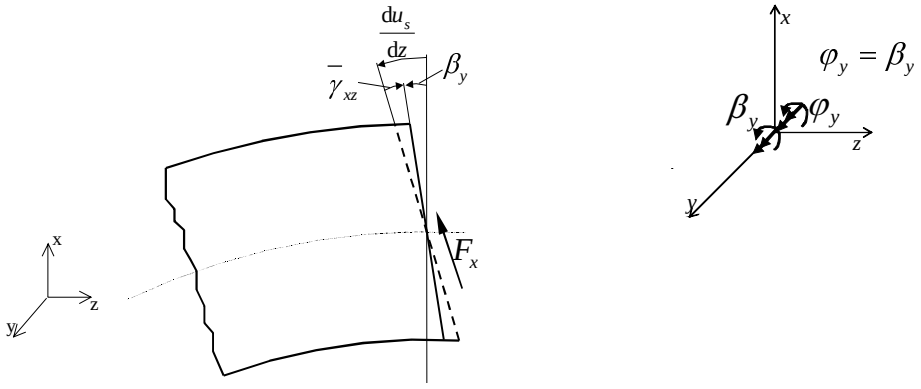

Fig. 1. Shear deformation in x-z plane.

Cross-sectional stress resultants generally consist of the axial force $F_z = \int_A \sigma_z \mathrm{d}A$, shear forces $F_x = \int_A \tau_{zx} \mathrm{d}A$ and $F_y = \int_A \tau_{zy} \mathrm{d}A$, torsional moment $M_z = \int_A [\tau_{zy}(x - x_s) - \tau_{zx}(y - y_s)] \mathrm{d}A$, bending moments $M_x = \int_A \sigma_z y \mathrm{d}A$ and $M_y = -\int_A \sigma_z x \mathrm{d}A$ and bimoment $M_\omega = \int_A \sigma_z \omega \mathrm{d}A$. The torsional moment is the sum of St.Venant's or uniform torsional moment T_{SV} and warping (or nonuniform) torsional moment T_ω. Due to restricted cross-sectional warping, an additional component, known as Wagner coefficient [2], appears. It can be expressed as

$$\overline{K} = \int_A \sigma_z \left[(x - x_s)^2 + (y - y_s)^2 \right] \mathrm{d}A \quad \text{or} \quad \overline{K} = \alpha_z F_z + \alpha_x M_x + \alpha_y M_y + \alpha_\omega M_\omega . \quad (6)$$

Detailed expressions of the coefficients $\alpha_z, \alpha_x, \alpha_y$ and α_ω can be found in [3]. When shear deformations due to F_x, F_y and T_ω are taken into account, we have

$$\frac{\mathrm{d}v_s}{\mathrm{d}z} + \varphi_x = \bar{\gamma}_{zy}, \qquad \frac{\mathrm{d}u_s}{\mathrm{d}z} - \varphi_y = \bar{\gamma}_{zx}, \qquad \frac{\mathrm{d}\varphi_s}{\mathrm{d}z} + \theta = \bar{\gamma}_\omega . \quad (7)$$

In the plane *x*-*z*, according to Fig. 1, we have

$$\frac{\mathrm{d}u_s}{\mathrm{d}z} - \beta_y = \frac{\mathrm{d}u_s}{\mathrm{d}z} - \varphi_y = \bar{\gamma}_{xz}, \quad M_y = EI_y \frac{\mathrm{d}\varphi_y}{\mathrm{d}z},$$
$$F_x = \bar{\tau}_{zx} A_x = G \bar{\gamma}_{xz} A_x = \frac{GA}{k_x} \left(\frac{\mathrm{d}u_s}{\mathrm{d}z} - \varphi_y \right), \quad (8)$$

and analogously for bending in *z*-*y* plane follows:

$$\frac{\mathrm{d}v_s}{\mathrm{d}z} - \beta_x = \frac{\mathrm{d}v_s}{\mathrm{d}z} + \varphi_x = \bar{\gamma}_{zy}, \quad M_x = EI_x \frac{\mathrm{d}\varphi_x}{\mathrm{d}z},$$
$$F_y = \bar{\tau}_{zy} A_y = G \bar{\gamma}_{zy} A_y = \frac{GA}{k_y} \left(\varphi_x + \frac{\mathrm{d}v_s}{\mathrm{d}z} \right), \quad (9)$$

and for torsion:

$$\frac{\mathrm{d}\varphi_z}{\mathrm{d}z}+\theta=\bar{\gamma}_\omega,\quad M_\omega=EI_\omega\frac{\mathrm{d}\theta}{\mathrm{d}z};\quad T_{SV}=GJ\frac{\mathrm{d}\varphi_z}{\mathrm{d}z},\quad T_\omega=G\bar{\gamma}_\omega J_\omega=\frac{GJ}{k_\omega}\left(\frac{\mathrm{d}\varphi_z}{\mathrm{d}z}+\theta\right). \tag{10}$$

In relations above, $\bar{\gamma}_{xz},\bar{\gamma}_{zy}$ and $\bar{\gamma}_\omega$ are average values of shear deformations, $\bar{\tau}_{xz}$ and $\bar{\tau}_{zy}$ are average values of shear stresses, A_x,A_y and J_ω are shear areas with respect to *x*, *y* and ω, and k_x,k_y and k_ω are flexible shear coefficients.

Flexible shear coefficients can be evaluated as

$$k_x=\frac{A}{I_y^2}\int_S C_y^2\frac{\mathrm{d}S}{t},\quad k_y=\frac{A}{I_x^2}\int_S C_x^2\frac{\mathrm{d}S}{t},\quad k_\omega=\frac{A}{I_\omega^2}\int_S C_\omega^2\frac{\mathrm{d}S}{t}, \tag{11}$$

where C_x,C_y and C_ω are first moments of the cross-section with respect to *x*, *y* and ω, defined as

$$C_y=\int_A x\mathrm{d}A=\int_0^S xt\mathrm{d}S,\quad C_x=\int_A y\mathrm{d}A=\int_0^S yt\mathrm{d}S,\quad C_\omega=\int_A \omega\mathrm{d}A=\int_0^S \omega t\mathrm{d}S. \tag{12}$$

2.2. The principle of virtual work

From the equilibrium between internal and external forces follows [4,5]:

$$\int_V S_{ij}\delta e_{ij}\mathrm{d}V+\int_V {}^0S_{ij}\delta\eta_{ij}\mathrm{d}V+\int_V {}^0S_{ij}\delta\tilde{e}_{ij}\mathrm{d}V-\int_{A_\sigma}{}^0t_i\delta\tilde{u}_i\mathrm{d}A_\sigma=\int_{A_\sigma}t_i\delta u_i\mathrm{d}A_\sigma. \tag{13}$$

Equation (14) is known as linearized principle of virtual work and it can be rewritten as [6]:

$$\delta \mathrm{U}_E+\delta \mathrm{U}_G-\delta W=\delta\Pi=0, \tag{14}$$

where $\delta \mathrm{U}_E$ is the elastic potential energy of internal forces, $\delta \mathrm{U}_G$ is the geometric potential of initial forces, $\delta \mathrm{W}$ is the virtual work of external forces and Π is total potential energy:

$$\delta \mathrm{U}_E=\int_V S_{ij}\delta e_{ij}\mathrm{d}V,$$

$$\delta \mathrm{U}_G=\int_{S_{ij}}{}^0S_{ij}\delta\eta_{ij}\mathrm{d}V+\int_V {}^0S_{ij}\delta\tilde{e}_{ij}\mathrm{d}V-\int_{A_\sigma}{}^0t_i\delta\tilde{u}_i\mathrm{d}A_\sigma,$$

$$\delta W=\int_{A_\sigma}t_i\delta u_i\mathrm{d}A_\sigma.$$

Introducing (1)–(6) into equations for $\delta \mathrm{U}_E$ and $\delta \mathrm{U}_G$ gives

$$\delta \mathrm{U}_E = \int_0^1 \Bigg[EA \frac{\mathrm{d}w_o}{\mathrm{d}z} \delta \frac{\mathrm{d}w_o}{\mathrm{d}z} + EI_x \frac{\mathrm{d}\varphi_x}{\mathrm{d}z} \delta \frac{\mathrm{d}\varphi_x}{\mathrm{d}z} + EI_y \frac{\mathrm{d}\varphi_y}{\mathrm{d}z} \delta \frac{\mathrm{d}\varphi_y}{\mathrm{d}z} + EI_\omega \frac{\mathrm{d}\theta}{\mathrm{d}z} \delta \frac{\mathrm{d}\theta}{\mathrm{d}z}$$
$$+ GJ \frac{\mathrm{d}\varphi_z}{\mathrm{d}z} \delta \frac{\mathrm{d}\varphi_z}{\mathrm{d}z} + \frac{GA}{k_y} \left(\frac{\mathrm{d}v_s}{\mathrm{d}z} - \varphi_x \right)^2 + \frac{GA}{k_x} \left(\frac{\mathrm{d}u_s}{\mathrm{d}z} + \varphi_y \right)^2$$
$$+ \frac{GJ}{k_\omega} \left(\frac{\mathrm{d}\varphi_z}{\mathrm{d}z} + \theta \right)^2 \Bigg] \mathrm{d}z, \tag{15}$$

$$\delta \mathrm{U}_G =$$
$$\frac{1}{2} \int_0^l \Bigg\{ {}^0F_z \left[\delta \left(\frac{\mathrm{d}w_o}{\mathrm{d}z} \right)^2 + \delta \left(\frac{\mathrm{d}v_s}{\mathrm{d}z} \right)^2 + \delta \left(\frac{\mathrm{d}u_s}{\mathrm{d}z} \right)^2 + 2y_s \delta \left(\frac{\mathrm{d}u_s}{\mathrm{d}z} \frac{\mathrm{d}\varphi_z}{\mathrm{d}z} \right) - 2x_{s\delta} \left(\frac{\mathrm{d}v_s}{\mathrm{d}z} \frac{\mathrm{d}\varphi_z}{\mathrm{d}z} \right) \right]$$
$$+ {}^0F_x \left[\delta(\varphi_x \varphi_z) + 2\delta \left(\frac{\mathrm{d}v_s}{\mathrm{d}z} \varphi_z \right) - 2\delta \left(\frac{\mathrm{d}w_o}{\mathrm{d}z} \varphi_y \right) + 2x_s \delta \left(\frac{\mathrm{d}\varphi_y}{\mathrm{d}z} \varphi_y \right) - 2y_s \delta \left(\frac{\mathrm{d}\varphi_x}{\mathrm{d}z} \varphi_y \right) \right]$$
$$+ {}^0F_y \left[\delta(\varphi_y \varphi_z) - 2\delta \left(\frac{\mathrm{d}u_s}{\mathrm{d}z} \varphi_z \right) + 2\delta \left(\frac{\mathrm{d}w_o}{\mathrm{d}z} \varphi_x \right) - 2x_s \delta \left(\frac{\mathrm{d}\varphi_y}{\mathrm{d}z} \varphi_x \right) - 2y_s \delta \left(\frac{\mathrm{d}\varphi_x}{\mathrm{d}z} \varphi_x \right) \right]$$
$$+ {}^0M_x \left[\delta \left(\frac{\mathrm{d}\varphi_y}{\mathrm{d}z} \varphi_z \right) + \delta \left(\frac{\mathrm{d}\varphi_z}{\mathrm{d}z} \varphi_y \right) - 2\delta \left(\frac{\mathrm{d}u_s}{\mathrm{d}z} \frac{\mathrm{d}\varphi_z}{\mathrm{d}z} \right) + 2\delta \left(\frac{\mathrm{d}w_o}{\mathrm{d}z} \frac{\mathrm{d}\varphi_x}{\mathrm{d}z} \right) \right]$$
$$+ {}^0M_y \left[-\delta \left(\frac{\mathrm{d}\varphi_x}{\mathrm{d}z} \varphi_z \right) - \delta \left(\frac{\mathrm{d}\varphi_z}{\mathrm{d}z} \varphi_x \right) - 2\delta \left(\frac{\mathrm{d}v_s}{\mathrm{d}z} \frac{\mathrm{d}\varphi_z}{\mathrm{d}z} \right) + 2\delta \left(\frac{\mathrm{d}w_o}{\mathrm{d}z} \frac{\mathrm{d}\varphi_y}{\mathrm{d}z} \right) \right]$$
$$+ {}^0M_z \left[\delta \left(\frac{\mathrm{d}\varphi_x}{\mathrm{d}z} \varphi_y \right) - \delta \left(\frac{\mathrm{d}\varphi_y}{\mathrm{d}z} \varphi_x \right) \right] + {}^0\overline{K} \, \delta \left(\frac{\mathrm{d}\varphi_z}{\mathrm{d}z} \right)^2 + {}^0M_\omega \left[\delta \left(\frac{\mathrm{d}w_o}{\mathrm{d}z} \frac{\mathrm{d}\theta}{\mathrm{d}z} \right) \right] \Bigg\} \mathrm{d}z. \tag{16}$$

3. FINITE ELEMENT OF THE THIN-WALLED BEAM

In Fig. 2 the finite element of the thin-walled beam with 14 degrees of freedom is shown [7,8]. The nodal displacement vector $\mathbf{u}^e$ and force vector $\mathbf{f}^e$ of an arbitrary *e*th element are:

$$(\mathbf{u}^e)^T = \{w_{oi} \; u_{si} \; v_{si} \; \varphi_{zi} \; \varphi_{xi} \; \varphi_{yi} \; \theta_i\}, \quad (\mathbf{f}^e)^T = \{F_{zi} \; F_{xi} \; F_{yi} \; M_{zi} \; M_{xi} \; M_{yi} \; M_{\omega i}\}. \tag{17}$$

For the finite element the equilibrium equation holds

$$(\mathbf{k}_E^e + \mathbf{k}_G^e)\mathbf{u}^e = \mathbf{f}^e, \tag{18}$$

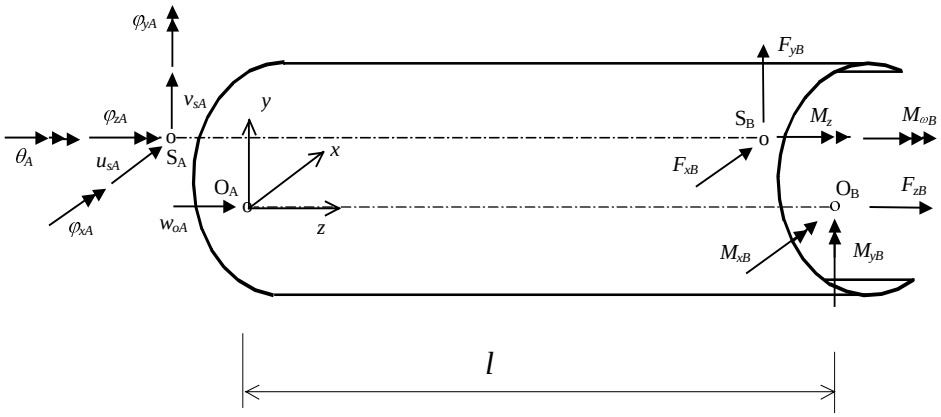

Fig. 2. Finite element of the thin-walled beam.

where $\mathbf{k}_E^e$ and $\mathbf{k}_G^e$ are elastic and geometric parts of the stiffness matrix in local coordinate system, which are obtained by solving integrals for $\delta \mathrm{U}_E$ and $\delta \mathrm{U}_G$ [9]. Interpolation functions for displacement components **w** are linear and for **u**, **v** and **φ** cubic interpolation is used. For the whole construction, equilibrium equation (assuming proportionality of loading) is

$$(\mathbf{K}_E + \lambda \hat{\mathbf{K}}_G)\,\mathbf{U} = \mathbf{F}, \tag{19}$$

where $\mathbf{K}_E$ is the elastic stiffness matrix of the construction, $\mathbf{K}_G$ is geometric stiffness matrix of the construction, **U** and **F** are vectors of incremental nodal displacements and nodal forces and λ is load parameter. Assuming that the external load does not change during the losing of stability $(\mathbf{F} = 0)$, Eq. (19) becomes

$$(\mathbf{K}_E + \lambda \hat{\mathbf{K}}_G)\,\mathbf{U} = 0. \tag{20}$$

Solving Eq. (20) for eigenvalues is called *linear stability analysis* [1] and eigenvalues $\lambda_1,\ldots,\lambda_n$ represent critical buckling loads. Only the first value λ_1 is of practical interest [10].

4. EXAMPLE

Computer program THINWALL-SHEAR, developed on the basis of the presented theory, is tested on a two examples.

4.1. Torsional-flexural buckling of a cantilever

A cantilever of unsymmetrical cross-section, loaded with axial force at the centroid, is shown in Fig. 3.

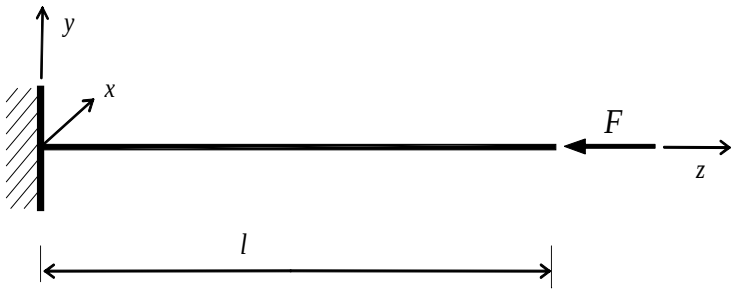

Fig. 3. Axially compressed cantilever of unsymmetrical cross-section (example 4.1).

Table 1. Values of F_{cr}(N) for the cantilever (example 4.1)

Number of elements	This paper	Kim et. al. [3]	ABAQUS [11]
1	13.9958		
2	13.8986	13.9017	14.0230
4	13.8930		

Material and geometrical parameters are the following: l = 200 cm, E = 30000 Ncm^{-2}, G = 11500 Ncm^{-2}; shear centre coordinates: x_s =1.58943 cm, y_s = –2.57228 cm; moments of inertia: I_x = 114.812 cm^4, I_y = 7.6048 cm^4; warping moment of inertia I_ω = 70.9687 cm^6; torsional moment of inertia J = 0.666667 cm^4; shear factors: k_x =5.2339, k_y =1.794438, k_ω = 0.01699; Wagner coefficients: α_x =5.66166 cm, α_y =11.0599cm, α_z =24.445 cm^2, α_ω = –0.558603. Values for critical buckling load F_{cr}, evaluated by program THINWALL-SHEAR are compared with the finite element results from [3], and with the results obtained with ABAQUS [11] (where an idealized cantilever with 1600 shell finite elements was used. Table 1 shows very good accuracy of the results obtained with ABAQUS.

4.2. Flexural buckling of a simply supported beam

The simply supported beam in Fig. 4 has doubly symmetric cross-section. The beam is axially loaded with compression force F . Due to double symmetry of the cross-section, the only possible buckling mode is flexural.

The relevant material and geometrical properties of the beam are: l = 100 cm, E = 2.1 × 10^7 Ncm^{-2}, G = 80.77 × 10^5 Ncm^{-2}; moments of inertia: I_x = I_y = 50 cm^4; cross-section area A = 5 cm^2. In Table 2, results obtained with program THINWALL-SHEAR are compared with numerical results and Timoshenko's analytical results, given in [3] for different values of the shear coefficient k = k_x = k_y. Table 2 shows very good coincidence of the results.

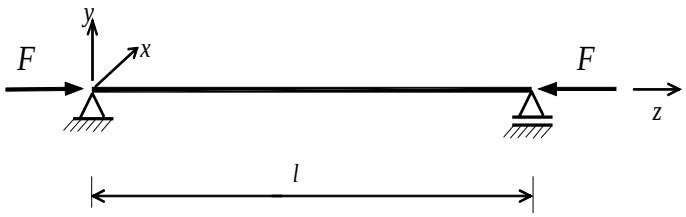

Fig. 4. Axially compressed simply supported beam of doubly symmetrical cross-section (example 4.2).

Table 2. Values of F_{cr} ($\times 10^{-6}$N) for flexural buckling of the beam under axial load

$\frac{k}{GA} F_{cr}$	THINWALL-SHEAR		Analytical (Timoshenko)	Kim et al. [3]
	Number of elements			
	2	4		
0	1.04410	1.03684	1.03630	1.03641
0.5	0.71541	0.69059	0.69087	0.69440
1	0.53516	0.51548	0.51815	0.52112
5	0.17193	0.16879	0.17272	0.17326
10	0.09254	0.09156	0.09421	0.09439
100	0.00992	0.00999	0.01026	0.01026
10 000	0.00010	0.00010	0.00010	0.00010

5. CONCLUSIONS

Numerical models are efficient alternatives for analytical modelling, which is applicable only in the case of very simple geometry of the structure. Presented numerical algorithm, based on the finite element method, includes large displacements and large rotations and also cross-sectional deformation effects. Coincidence of the results, obtained with the program THINWALL-SHEAR for two typical examples, with the results of other authors available from literature, encourages application of numerical models to problems of more complex constructions.

REFERENCES

1. Yang, Y. B. and Kuo, S. R. *Theory and Analysis of Nonlinear Framed Structures.* Prentice Hall, New York, 1994.
2. Kim, M. Y., Chang, S. P. and Kim, S. B. Spatial postbuckling analysis of thin-walled frames II: geometrically nonlinear FE procedures. *J. Eng. Mech.*, 2001, **127**, 779–790.
3. Kim, M. Y., Chang, S. P. and Kim, S. B. Spatial stability and free vibration of shear flexible thin-walled elastic beams II: numerical approach. *Int. J. Numer. Meth. Eng.*, 1994, **37**, 4117–4140.
4. Turkalj, G., Brnic, J. and Prpic-Orsic, J. Large rotation analysis of elastic thin-walled beam-type structures using ESA approach, *Comput. Struct.*, 2003, **81**, 1851–1864.

5. Turkalj, G., Brnic, J. and Prpic-Orsic, J. External stiffness approach for thin-walled frames with elastic-plasticity. In *Proc. Sixth International Conference on Computational Structures Technology*. (Topping, B. H. V. and Bittnar, Z., eds.), Prague, 2000. Civil-Comp Press, Stirling, 2002, 67–68.
6. Chang, S. P., Kim, S. B. and Kim, M. Y. Stability of shear deformable thin-walled space frames and circular arches. *J. Eng. Mech.*, 1996, **122**, 844–854.
7. Bathe, K. J. *Finite Element Procedure*. Prentice Hall, London, 1996.
8. Mihanovic, A. *Stabilnost Konstrukcija*. Hrvatsko drustvo gradevinskih konstruktora, Zagreb, 1993 (in Croatian).
9. Turkalj, G. and Brnic, J. Analiza elastičnog izvijanja tankostijenih grednih konstrukcija s obzirom na velike rotacije. *Strojarstvo*, 2000, **42**, 217–230 (in Croatian).
10. Turkalj, G., Brnic, J. and Lanc, D. Elastic-plastic large displacement analysis of thin-walled beam type structures. In *System-based Vision for Strategic and Creative Design* (Bontempi, F., ed.). Balkema, Lisse, 2003, 639–644.
11. Turkalj, G., Brnic, J. and Lanc, D. Non-linear formulation for elastic stability analysis of thin-walled beam-type structures. In *Metal Structures: Design, Fabrication, Economy*, (Jarmai, K. and Farkas, J., eds.). Millpress, Rotterdam, 2003, 79–86.

Õhukeseseinaliste talade nihkedeformeerumise lineaarne stabiilsusanalüüs

Domagoj Lanc, Goran Turkalj ja Josip Brnić

Töös käsitletakse analüütiliselt ja lõplike elementide meetodil õhukeseseinaliste talade stabiilsust nihkedeformeerumisel. Viimase arvutamiseks on välja töötatud programm.